

See discussions, stats, and author profiles for this publication at: <https://www.researchgate.net/publication/237885438>

# Existence of a Hydroperoxy and Water ( $\text{HO}_2 \cdot \text{H}_2\text{O}$ ) Radical Complex

ARTICLE in THE JOURNAL OF PHYSICAL CHEMISTRY A · MARCH 1998

Impact Factor: 2.69 · DOI: 10.1021/jp972173p

---

CITATIONS

127

---

READS

26

2 AUTHORS, INCLUDING:



Simone Aloisio

California State University, Channel Islands

37 PUBLICATIONS 979 CITATIONS

SEE PROFILE

# Existence of a Hydroperoxy and Water ( $\text{HO}_2\cdot\text{H}_2\text{O}$ ) Radical Complex

S. Aloisio and J. S. Francisco\*

Department of Chemistry and Department of Earth and Atmospheric Sciences, Purdue University, West Lafayette, Indiana 47907-1393

Received: July 3, 1997; In Final Form: December 4, 1997

The structure, vibrational spectrum, and binding energy of  $\text{HO}_2\cdot\text{H}_2\text{O}$  are predicted using ab initio molecular methods. Theory predicts that the  $\text{HO}_2\cdot\text{H}_2\text{O}$  complex is bound by  $6.9 \text{ kcal mol}^{-1}$ . The equilibrium structure and rotational constants of the complex have been determined. The OH stretching frequency of the  $\text{HO}_2$  is red-shifted by  $296 \text{ cm}^{-1}$  from the isolated molecule. Its infrared intensity is also enhanced by 22 times that of the monomer.

## I. Introduction

Despite the fact that many measurements of weakly bound species have been made in the laboratory, little is known of the role these species play in the chemistry of the atmosphere. Recently, experimental<sup>1</sup> and theoretical studies<sup>2</sup> of the  $\text{SO}_3\cdot\text{H}_2\text{O}$  complex have shown that such species can act to enhance reaction rates. A  $\text{ClO}\cdot\text{H}_2\text{O}$  complex has been suggested to enhance the rate of ClO dimer formation.<sup>3</sup> Studies by Frost and Vaida<sup>4</sup> have shown that photodissociation of  $\text{O}_3\cdot\text{H}_2\text{O}$  complexes can lead to the production of more  $\text{O}(^1\text{D})$ , which would lead to the formation of more OH radicals in the troposphere. The role the  $\text{HO}_x$  family plays (OH and  $\text{HO}_2$  radicals) is quite important with regard to stratospheric ozone chemistry. Moreover, these species are important in tropospheric oxidation processes. In regions of the atmosphere where the temperature is low or where water-vapor concentration is high, the atmospheric conditions are such that the formation of an association complex, i.e.,  $\text{HO}_2\cdot\text{H}_2\text{O}$ , is likely. The existence of an  $\text{HO}_2\cdot\text{H}_2\text{O}$  complex has been suggested from previous laboratory studies<sup>5–8</sup> in which the complex has been suggested to enhance the rate of  $\text{H}_2\text{O}_2$  formation by as much as a factor of 3. To date, no study has been reported on the experimental detection of an  $\text{HO}_2\cdot\text{H}_2\text{O}$  complex. In this paper, we use ab initio calculations to determine the stability of the  $\text{HO}_2\cdot\text{H}_2\text{O}$  complex and provide some predictions of its vibrational and rotational spectra that could facilitate the experimental characterization of the complex. We estimate the equilibrium constant for the formation of the complex from the results of the calculations, which is then used to assess if such complexes could be formed in sufficient quantity to play a role in the chemistry of the atmosphere.

## II. Computational Methods

All calculations were performed using GAUSSIAN 94.<sup>9</sup> Geometries for the  $\text{HO}_2\cdot\text{H}_2\text{O}$  complex were optimized with unrestricted second-order Møller–Plesset theory (UMP2).<sup>10,11</sup> They were also done with the Becke's nonlocal three-parameter exchange and correlation functional<sup>12</sup> with the Lee–Yang–Parr correlation functional method (B3LYP).<sup>13</sup> Calculations were performed with a range of medium-to-large basis sets such as 6-31G(d), 6-31++G(d), 6-311++G(d), 6-311++G(d,p), 6-311++G(2d,2p), 6-311++G(2df,2p), and 6-311++G(3df,3pd).<sup>14,15</sup> Single-point energy calculations were done using the

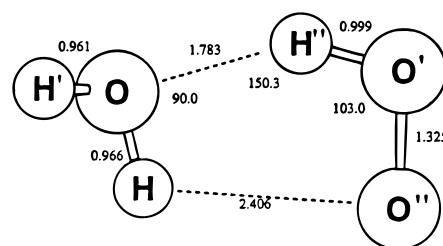


**Figure 1.** Optimized structure for  $\text{HO}_2\cdot\text{H}_2\text{O}$  radical complex. Distances are in angstroms and bond angles are in degrees. The numbers are calculated at the B3LYP/6-311++G(3df,3pd) level of theory. The full geometry can be obtained from the supplemental table.

unrestricted coupled cluster method including single and double excitation and including perturbational estimates of the effects of connected triple excitation [CCSD(T)].<sup>16,17</sup> Vibrational frequencies and zero-point energies for the complexes and their respective monomers were calculated using both MP2 and B3LYP methods. Basis set superposition errors were calculated by applying the full Boys–Bernardi counterpoise correction scheme.<sup>18</sup>

## III. Results and Discussion

Other researchers<sup>19,20</sup> performed initial ab initio calculations of the  $\text{HO}_2\cdot\text{H}_2\text{O}$  complex using an ST0-3G<sup>19,20</sup> and the 4-31G<sup>20</sup> basis set. Their study did not use a fully optimized structure, only a constrained structure. The authors did not perform a frequency calculation on their structure to verify if it was indeed a true minima. We found that the Hamilton and Naleway<sup>19</sup> structure was a saddle point. In that structure, the oxygen of the water  $\text{H}_2\text{O}$  and the hydrogen and middle oxygen of the  $\text{HO}_2$  are constrained to be collinear. Also, the hydrogen-bond axis is constrained to be in the  $\sigma_v$  plane of the water, which fixes the hydrogen atoms of the water to be symmetrical with respect to the hydrogen bond. This does not allow these hydrogen atoms to interact with the terminal oxygen on the  $\text{HO}_2$  molecule. Rao et al.<sup>20</sup> used a similar structure in their calculation. Figure 1 depicts the most stable conformer we found for the  $\text{HO}_2\cdot\text{H}_2\text{O}$  complex. In the complex, the hydrogen from the  $\text{HO}_2$  is weakly bound to the oxygen from the water. There is also an attractive interaction between the terminal oxygen in the peroxy radical and one of the hydrogens on the water. This causes the structure to have a floppy five-membered

**TABLE 1: Geometry of Complexes B3LYP and MP2<sup>a</sup>**

basis set	bond lengths						bond angles				dihedrals		
	R	O''H	HO	H'O	H''O'	O'O''	HOH'	H'OH''	OH''O'	H''O'O''	dHH'OH''	dH'OH''O'	dOH''O'O''
(a) B3LYP													
6-31G(d)	1.761	2.102	0.978	0.970	1.004	1.331	104.6	81.9	144.6	102.6	250.5	359.0	2.9
6-31++G(d)	1.765	2.638	0.972	0.970	0.999	1.334	108.2	97.6	154.7	103.5	135.8	359.5	1.4
6-311++G(d)	1.742	2.893	0.964	0.963	0.991	1.328	108.2	107.1	158.6	104.7	220.2	359.2	0.9
6-311++G(d,p)	1.774	2.627	0.965	0.962	0.992	1.328	106.5	99.1	152.8	103.9	227.1	354.9	3.8
6-311++G(2d,2p)	1.791	2.404	0.966	0.961	0.991	1.328	106.2	90.1	149.6	103.5	237.0	354.4	4.2
6-311++G(2df,2p)	1.796	2.425	0.966	0.961	0.991	1.325	106.3	90.9	149.6	103.7	235.1	354.6	3.9
6-311++G(3df,3pd)	1.781	2.406	0.966	0.961	0.999	1.325	106.1	90.0	150.3	103.0	235.9	354.3	4.3
(b) MP2													
6-31G(d)	1.893	2.895	0.949	0.948	0.960	1.310	106.2	102.0	157.3	104.6	232.5	356.5	11.6
6-31++G(d)	1.778	2.833	0.974	0.973	0.997	1.323	105.9	101.8	159.3	103.3	232.6	358.7	2.1
6-311++G(d)	1.759	3.047	0.960	0.959	0.982	1.304	108.4	111.7	161.2	105.1	210.5	357.5	1.8
6-311++G(d,p)	1.766	2.927	0.961	0.960	0.983	1.306	104.7	106.7	160.5	103.7	225.0	357.3	4.6
6-311++G(2d,2p)	1.783	2.536	0.962	0.958	0.983	1.312	105.3	93.3	153.7	103.1	235.2	354.4	4.5
6-311++G(2df,2p)	1.789	2.535	0.962	0.958	0.990	1.301	104.9	91.4	152.9	103.5	251.1	354.9	4.5

<sup>a</sup> All bond distances are reported in angstroms. All bond angles and dihedrals are reported in degrees.

**TABLE 2: Rotational Constants for the HO<sub>2</sub>·H<sub>2</sub>O Complex**

	rotational constants <sup>a</sup>		
	A	B	C
UMP2/6-311++G(2d,2p)	33 325	5706	4921
B3LYP/6-311++G(2d,2p)	32 186	5859	5009
UMP2/6-311++G(2df,2p)	33 528	5861	5036
B3LYP/6-311++G(2df,2p)	32 375	5824	4986
B3LYP/6-311++G(3df,3pd)	32 510	5862	5018

<sup>a</sup> All rotational constants are reported in MHz.

ring like structure with an additional hydrogen from the water out of the plane. The bond distances and angles are listed in Table 1. We did explore other structures on the HO<sub>2</sub>·H<sub>2</sub>O potential energy surface but found that these structures were not local or global minimas.

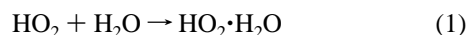
We used two different optimization methods in order to explore the potential energy surface to look for minima. The first is the second-order Møller–Plessett perturbation method, and the second is the B3LYP density functional theory method. We used a range of basis sets, from the 6-31G(d) to the 6-311++G(3df,3pd). Both methods yielded similar geometries. Del Bene et al.<sup>21</sup> found that density functional B3LYP/6-31G(d,p) calculations fail to yield reliable intermolecular distances for selected closed-shell hydrogen-bonded complexes. They did, however, find that the addition of diffuse functions improved the agreement but generally found that MP2 results were better. In the present study of HO<sub>2</sub>···H<sub>2</sub>O, we have performed calculations with both B3LYP and MP2 methods. We find that with the 6-31G(d,p) and the 6-31++G(d) basis sets there are very large differences in the geometry for the intermolecular distances as suggested by Del Bene et al.<sup>21</sup> For example the O''H bond distance is 2.102 Å at the B3LYP/6-31G(d) level, while at the MP2/6-31G(d) level it is 2.895 Å. However, with the large basis sets we find that the results for the MP2 and B3LYP converge. We also performed frequency calculations using these levels of theory and basis sets. The density functional theory method seemed to provide frequencies and intensities closer to those published in the case of the isolated monomers.

The rotational constants for the optimized structure at various levels of theory are reported in Table 2. From the rotational constants, as well as the structure, it is evident that the molecule is an asymmetric rotor. The rotational constants show that spectroscopically HO<sub>2</sub>···H<sub>2</sub>O will almost behave like an oblate symmetric rotor because  $B_A > B_B \approx B_C$ . Since this molecule has a permanent dipole moment, it should be active in the

microwave region of the spectrum. This information is useful in characterizing the rotational and the rovibrational spectra of the HO<sub>2</sub>·H<sub>2</sub>O complex.

The calculated binding energies for the HO<sub>2</sub>·H<sub>2</sub>O complex are given in Table 3. Using the 6-311++G(2d,2p) basis set, we find the predicted  $D_e$  to be 9.4 kcal mol<sup>-1</sup> for UMP2 and 8.9 kcal mol<sup>-1</sup> for B3LYP methods. Extension of the basis set to the large 6-311++G(3df,3pd) modestly decreases the predicted  $D_e$  to 8.8 kcal mol<sup>-1</sup>. This is consistent with the small structural charges between 6-311++G(2d,2p) and 6-311++G(3df,3pd) optimized geometries. The binding energy for HO<sub>2</sub>·H<sub>2</sub>O predicts that the complex is more tightly bound than the HO·H<sub>2</sub>O complex,<sup>22,23</sup> which has an estimated  $D_e$  of 5.6 kcal mol<sup>-1</sup>. It is also higher than the HO<sub>2</sub>·H<sub>2</sub>O dimer binding energy studied by Rao et al.<sup>20</sup> At the highest level of theory, CCSD(T)/6-311++G(2df,2p)//B3LYP/6-311++G(2df,2p), the  $D_e$  is 9.4 kcal mol<sup>-1</sup> for HO<sub>2</sub>·H<sub>2</sub>O. Corrections for vibrational zero-point energy yield a value of  $D_0$  of 6.9 kcal mol<sup>-1</sup>. This correction is probably exaggerated because the vibrational zero-point energy correction is calculated in the harmonic approximation, while the actual potential energy surface for the HO<sub>2</sub>·H<sub>2</sub>O is anharmonic. The basis set superposition error for this energy calculation is estimated to be 1.0 kcal mol<sup>-1</sup>. With such large binding energies, these calculations suggest that the HO<sub>2</sub>·H<sub>2</sub>O complex should be experimentally observable.

Using the experimental binding energy and the thermal energy, we computed the change in enthalpy,  $\Delta H$ , and the change in entropy,  $\Delta S$ , at 298 K for reaction 1:



The change in enthalpy was calculated using the difference in the electronic and thermal energies of the products and reactants using the following equation

$$\Delta H = (\Delta E_e + \Delta E_{\text{th}})_{\text{prod.}} - (\Delta E_e + \Delta E_{\text{th}})_{\text{react.}} - RT \quad (2)$$

where  $\Delta E_e$  is the electronic energy;  $\Delta E_{\text{th}}$  is the thermal energy, which includes the translational, rotational, and vibrational energies; and the  $-RT$  term is included because 1 mol of gas is being lost in this reaction. The enthalpy change we calculated is  $-7.6$  kcal mol<sup>-1</sup>. This is similar to the enthalpy change calculated by Hamilton and Naleway of  $-7.4$  kcal mol<sup>-1</sup>, in which the authors estimated the vibrational energy of the complex by using the data available for the water dimer. The change in entropy at 298 K has been calculated to be  $-25.5$

**TABLE 3: HO<sub>2</sub>·H<sub>2</sub>O Complex Binding Energy**

levels of theory	HO <sub>2</sub> ·H <sub>2</sub> O		HO <sub>2</sub>		H <sub>2</sub> O		binding energy <sup>b</sup>	
	energy <sup>a</sup>	ZPE corrected	energy <sup>a</sup>	ZPE corrected	energy <sup>a</sup>	ZPE corrected	D <sub>e</sub>	D <sub>0</sub>
UMP2/6-311++G(2d,2p)	-227.0048	-226.9644	-150.6725	-150.6579	-76.3174	-76.2957	9.4	6.8
B3LYP/6-311++G(2d,2p)	-227.4401	-227.4004	-150.9639	-150.9497	-76.4620	-76.4407	8.9	6.3
UMP2/6-311++G(2df,2p)	-227.0639	-227.0235	-150.7124	-150.6978	-76.3362	-76.3145	9.6	7.0
B3LYP/6-311++G(2df,2p)	-227.4435	-227.4039	-150.9668	-150.9526	-76.4626	-76.4413	8.8	6.3
B3LYP/6-311++G(3df,3pd)	-227.4469	-227.4073	-150.9683	-150.9542	-76.4645	-76.4432	8.8	6.2
CCSD(T)/6-311++G(2df,2p)	-227.0468	-227.0072	-150.7035	-150.6894	-76.3282	-76.3069	9.4	6.9

<sup>a</sup> Single point calculated with the B3LYP/6-311++G(2df,2p) geometry. <sup>b</sup> Binding energies are in kcal mol<sup>-1</sup>.

**TABLE 4: Harmonic Vibrational Frequencies (cm<sup>-1</sup>) and Intensities (km mol<sup>-1</sup>) for the HO<sub>2</sub>·H<sub>2</sub>O Complex**

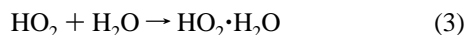
mode no.	mode description	frequency (cm <sup>-1</sup> ) [shift (cm <sup>-1</sup> )] <sup>a</sup>			intensity (km mol <sup>-1</sup> ) <sup>b</sup>		
		UMP2/ 6-311++G(2d,2p)	B3LYP/ 6-311++G(2d,2p)	B3LYP/ 6-311++G(3df,3pd)	UMP2/ 6-311++G(2d,2p)	B3LYP/ 6-311++G(2d,2p)	B3LYP/ 6-311++G(3df,3pd)
1	HO(HOH') asym str.	3957 (-30)	3892 (-32)	3871 (-43)	111 (1.5)	103 (1.7)	103 (1.7)
2	HO(HOH') sym str.	3835 (-32)	3773 (-49)	3752 (-62)	28 (2.8)	36 (5.1)	33 (5.5)
3	H''O' str.	3455 (-256)	3338 (-278)	3306 (-296)	584 (11)	536 (18)	533 (22)
4	HOH' bend	1664 (+2)	1640 (+1)	1625 (+2)	67 (1.0)	69 (0.97)	67 (0.93)
5	H''O'O'' bend	1588 (+119)	1566 (+125)	1556 (+120)	64 (2.2)	84 (2.2)	83 (2.1)
6	O'O'' str.	1281 (+60)	1193 (+26)	1183 (+14)	92 (0.93)	20 (0.69)	19 (0.70)
7	H'OH'' bend	694	686	679	163	161	140
8	HOH bend	447	479	465	85	108	94
9	OH''O bend	296	306	293	154	134	131
10	OH'' str.	254	256	255	16	25	24
11	HOH'H' torsion	174	208	103	64	71	69
12	OH''O'O'' torsion	79	101	98	34	45	47

<sup>a</sup> Numbers in parentheses are calculated shifts relative to the monomers. <sup>b</sup> Numbers in parentheses are ratios of calculated intensities for the complex relative to the monomers.

cal mol<sup>-1</sup> K<sup>-1</sup>. This agrees fairly well with Hamilton and Naleway's calculation of -24.5 cal mol<sup>-1</sup> K<sup>-1</sup>.

In Table 4 the harmonic vibrational frequencies for the HO<sub>2</sub>·H<sub>2</sub>O radical complex are shown. By using the B3LYP/6-311++G(3df,3pd) level of theory, we were able to predict the vibrational frequencies of HO<sub>2</sub> within a root-mean-square error of 6.1% of the experiment<sup>24-26</sup> and intensities within a factor of 4. This is consistent with previous density functional theory studies on HO<sub>2</sub>.<sup>27</sup> The frequency shifts are calculated by taking the difference between the vibrational frequencies of the isolated H<sub>2</sub>O and HO<sub>2</sub> molecules and the radical complex using the same basis set and the same level of theory. At the MP2 and B3LYP levels of theory using 6-311G(2d,2p) and 6-311++G(3df,3pd) basis sets, the shift between the levels of theory are consistently predicted in terms of magnitude and sign. The largest shift results in the H''O' stretching mode that is red-shifted by 296 cm<sup>-1</sup>. The intensity of this mode is predicted to be 22 times greater than that of the isolated HO<sub>2</sub> at the best level of theory. This is because of the increased effect this mode has on the change in the dipole moment of the entire complex. On the HO<sub>2</sub> moiety, the H''O'O'' bending mode is blue-shifted by 120 cm<sup>-1</sup>. The calculations predict the H''O' stretching mode ( $\nu_3$ ) in the complex to be the most intense band. There are six intermolecular modes, whose frequencies are well-separated from those of the isolated monomers. These are modes  $\nu_7$  through  $\nu_{12}$ . The  $\nu_7$  and  $\nu_9$  modes, in particular, are predicted to be intense modes. The observation of these vibrational modes in the laboratory could support the existence of the HO<sub>2</sub>·H<sub>2</sub>O radical complex.

The equilibrium constant for the following reaction



is estimated from partition functions using statistical thermodynamics.<sup>28</sup> The transitional, vibrational, rotational, and electronic partition functions are calculated from the ab initio

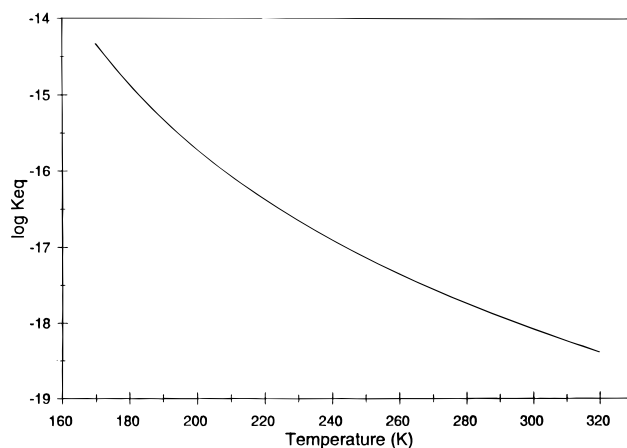


**Figure 2.** HO<sub>2</sub>·H<sub>2</sub>O equilibrium constant as a function of temperature.  $K_{eq}$  is in units of cm<sup>3</sup> molecule<sup>-1</sup>.

structural, vibrational, and binding energy data given. The equilibrium constant, which is in units of cm<sup>3</sup> molecule<sup>-1</sup>, is found by dividing the total partition function of the product HO<sub>2</sub>·H<sub>2</sub>O by the total partition functions of the reactants, HO<sub>2</sub> and H<sub>2</sub>O. The equation for this calculation, as given in reference 28, is

$$K_c(T) = \rho_{\text{HO}_2\cdot\text{H}_2\text{O}} / \rho_{\text{HO}_2} \rho_{\text{H}_2\text{O}} \quad (4)$$

where  $K_c(T)$  is the temperature-dependent equilibrium constant in terms of concentration and  $\rho_{\text{HO}_2\cdot\text{H}_2\text{O}}$ ,  $\rho_{\text{HO}_2}$ , and  $\rho_{\text{H}_2\text{O}}$  are the total partition functions of the reactants and product of reaction 1. The equilibrium constant for HO<sub>2</sub>·H<sub>2</sub>O is calculated to range from 170 to 320 K and is shown in Figure 2. At the higher temperatures the equilibrium constant is estimated to be on the order of 10<sup>-18</sup>, while at lower temperatures it increases by 3 orders of magnitude. Consequently, lower temperatures will

favor the complex formation. The largest source of uncertainty lies in the determination of the binding energy of the complex. For the equilibrium constant calculation, we used the binding energy calculated by the CCSD(T)/6-311++G(2df,2p)//B3LYP/6-311++G(2df,2p) level of theory. Using water dimer as a benchmark calculation, the  $D_0$  at the same level of theory is found to be within 0.2% of the experimentally determined binding energy.<sup>29</sup> This translates into an error in the equilibrium constant of about 1.2%. The calculated vibrational frequencies reported in Table 4 are harmonic values; consequently, we need to estimate the uncertainty in the equilibrium constant due to the effect of anharmonic corrections for the frequencies. We used a procedure similar to that of Feyereisen et al.<sup>30</sup> First we compared the calculated frequencies of the monomers, HO<sub>2</sub> and H<sub>2</sub>O, to experimental values. An average scale factor of 0.983 for the stretches and 0.977 for the bend were obtained. These scale factors were used for the monomer modes of the dimer. We did not vary the six intermolecular modes of the dimers. We recalculated the equilibrium constant using the scaled vibrational frequencies. An estimate of the error in the equilibrium constant due to the neglect of anharmonicity is <0.5%. Thus, there are no large effects contributing to the equilibrium constant estimation from the anharmonic corrections.

We have asked the question in what regions of the atmosphere are HO<sub>2</sub>·H<sub>2</sub>O complexes most likely to be formed. In regions where the water concentration is low, it seems unlikely that these complexes could be formed in significant number density to have any impact. For example, in the stratosphere at 30 km, the H<sub>2</sub>O concentration is  $1.6 \times 10^{12}$  molecules cm<sup>-3</sup>, the HO<sub>2</sub> density is  $1.6 \times 10^7$  molecules cm<sup>-3</sup>, and the mean temperature at this altitude is 232.1 K.<sup>31</sup> This implies that  $5.2 \times 10^2$  HO<sub>2</sub>·H<sub>2</sub>O complexes should exist in a column of  $1.6 \times 10^7$  HO<sub>2</sub> molecules. However, where these species could play a role in the atmosphere is in the marine boundary layer and in the tropical troposphere. In the marine boundary layer,<sup>32</sup> the water density is  $2.6 \times 10^{17}$  molecules cm<sup>-3</sup>, the mean temperature is 283.4 K, and the HO<sub>2</sub> density is  $2.7 \times 10^8$  molecules cm<sup>-3</sup>. Under these conditions we estimate that  $1.1 \times 10^8$  HO<sub>2</sub>·H<sub>2</sub>O complexes exist; in other words, 29% of the HO<sub>2</sub> is complexed as HO<sub>2</sub>·H<sub>2</sub>O. Although the equilibrium constant for complex formation decreases with increasing temperature, the amount of water in the atmosphere may increase dramatically at these higher temperatures. For this reason, larger amounts of the HO<sub>2</sub>·H<sub>2</sub>O complex may be formed in areas where the temperature is higher, such as in the tropics. Let us, as an example, take a warmer air mass with a temperature of 298 and a humidity of 80% ( $7.8 \times 10^{17}$  molecules cm<sup>-3</sup> of H<sub>2</sub>O). In this region, using the same HO<sub>2</sub> concentration as above, 42% of the HO<sub>2</sub> could be in the complexed form. Given the various points of uncertainty in the estimation of the equilibrium constant, the present results suggest that HO<sub>2</sub>·H<sub>2</sub>O complexes should exist in significant abundance in the lower region of the atmosphere where conditions of high water density and low temperature should favor its formation. As a result, it would be interesting to know what the implications of such abundances of HO<sub>2</sub>·H<sub>2</sub>O complexes may have on the chemistry of the atmosphere.

**Note Added in Proof.** Subsequent to the submission of this paper, Nelander<sup>33</sup> submitted a paper on the matrix isolation of the HO<sub>2</sub>·H<sub>2</sub>O complex in which vibrational frequencies were reported. The three major fundamental vibrational bands reported are at 3236.2, 1479.3, and 1120.4 cm<sup>-1</sup>. These are in good agreement with our best predictions at 3306, 1556, and

1183 cm<sup>-1</sup>. Our calculations deviate by 2.1%, 5.2%, and 5.6% from the experimental values, respectively. Nelander assigns these modes as  $\nu_1$ ,  $\nu_2$ , and  $\nu_3$ , respectively. However, the present work suggest that these modes are attributed to  $\nu_3$ ,  $\nu_5$ , and  $\nu_6$  for the HO<sub>2</sub>·H<sub>2</sub>O complex. Nelander suggested that the binding energy of the HO<sub>2</sub>·H<sub>2</sub>O complex is at least 6 kcal mol<sup>-1</sup>, which is in good agreement with our estimate of 6.9 kcal mol<sup>-1</sup>. The results of Nelander<sup>33</sup> provide confirmation of the present calculations of the existence of the HO<sub>2</sub>·H<sub>2</sub>O radical complex.

**Acknowledgment.** We thank Drs. S. P. Sander and Y. Yung for several important discussions during the course of this work. The Cray Supercomputer used in the investigation was provided by funding from the NASA Office of Mission to Planet Earth, Aeronautics, and Space Science.

## References and Notes

- (1) Kolb, C. E.; Jayne, J. T.; Worsnop, D. R.; Molina, M. J.; Meads, R. F.; Viggiano, A. A. *J. Am. Chem. Soc.* **1994**, *116*, 10314.
- (2) Morokuma, K.; Muguruma, C. *J. Am. Chem. Soc.* **1994**, *116*, 10316.
- (3) Francisco, J. S.; Sander, S. P. *J. Am. Chem. Soc.* **1995**, *117*, 9917.
- (4) Frost, G. J.; Vaida, V. *J. Geophys. Res.* **1995**, *100*, 18803.
- (5) Hamilton, E. J. *J. Chem. Phys.* **1975**, *63*, 3682.
- (6) Cox, R. A.; Burrows, J. P. *J. Phys. Chem.* **1979**, *83*, 2560.
- (7) Lii, R. R.; Grose, R. A.; Sauer, M. C.; Gordon, S. *J. Phys. Chem.* **1980**, *84*, 813.
- (8) Kircher, C. C.; Sander, S. P. *J. Phys. Chem.* **1984**, *88*, 2082.
- (9) Frisch, M. J.; Trucks, G. W.; Schlegel, H. B.; Gill, P. M. W.; Johnson, B. G.; Robb, M. A.; Cheeseman, J. R.; Keith, T.; Petersson, G. A.; Montgomery, J. A.; Raghavachari, K.; Al-Laham, M. A.; Zakrzewski, V. G.; Ortiz, J. V.; Foresman, J. B.; Peng, C. Y.; Ayala, P. Y.; Chen, W.; Wong, M. W.; Andres, J. L.; Replogle, E. S.; Gomperts, R.; Martin, R. L.; Fox, D. J.; Binkley, J. S.; Defrees, D. J.; Baker, J.; Stewart, J. P.; Head-Gordon, M.; Gonzalez, C.; Pople, J. A. *Gaussian 94*, Revision B.3; Gaussian, Inc.: Pittsburgh, PA, 1995.
- (10) Möller, C.; Plesset, M. S. *Phys. Rev.* **1934**, *46*, 618.
- (11) Frisch, M. J.; Head-Gordon, M.; Pople, J. A. *J. Chem. Phys.* **1990**, *141*, 189.
- (12) Becke, A. D. *J. Chem. Phys.* **1993**, *98*, 1372, 5648.
- (13) Lee, C.; Yang, W.; Parr, R. G. *Phys. Rev. B* **1988**, *41*, 785.
- (14) Ditchfield, R.; Hehre, W. J.; Pople, J. A. *J. Chem. Phys.* **1971**, *54*, 724.
- (15) Frisch, M. J.; Pople, J. A.; Binkley, J. S. *J. Chem. Phys.* **1984**, *80*, 3265.
- (16) Purvis, G. D., III; Bartlett, R. J. *J. Chem. Phys.* **1982**, *76*, 1910.
- (17) Lee, T. J.; Rendell, A. P. *J. Chem. Phys.* **1991**, *69*, 399.
- (18) Boys, S. F.; Bernardi, F. *Mol. Phys.* **1970**, *19*, 553.
- (19) Hamilton, E. J.; Naleway, C. A. *J. Phys. Chem.* **1976**, *80*, 2037.
- (20) Rao, C. N. R.; Kulkarni, G. V.; Rao, A. M.; Singh, U. C. *J. Mol. Struct.* **1984**, *198*, 113.
- (21) Del Bene, J. E.; Person, W. B.; Szczepaniak, K. *J. Phys. Chem.* **1995**, *99*, 10705.
- (22) Kim, K. S.; Kim, H. S.; Jung, J. H.; Mhin, B.-J.; Xie, Y.; Schaefer, H. F., III. *J. Chem. Phys.* **1991**, *94*, 2057.
- (23) Xie, Y.; Schaefer, H. F., III. *J. Chem. Phys.* **1993**, *98*, 8829.
- (24) Zahniser, M. S.; McCurdy, K. F.; Stanton, A. C. *J. Phys. Chem.* **1989**, *93*, 1065.
- (25) Nelson, D. D.; Zahniser, M. S. *J. Mol. Spectrosc.* **1991**, *1150*, 527.
- (26) Zahniser, M. S.; Stanton, A. C. *J. Chem. Phys.* **1984**, *80*, 4951.
- (27) Dobbs, K. D.; Dixon, D. A. *J. Phys. Chem.* **1994**, *98*, 4498.
- (28) McQuarrie, D. A. *Statistical Thermodynamics*; Harper and Row: New York, 1973.
- (29) At the CCSD(T)/6-311++G(2df,2p)//B3LYP/6-311++G(2df,2p) level of theory, the binding energy for the water dimer was calculated to be 5.39 kcal mol<sup>-1</sup>. The value was reported to be  $5.4 \pm 0.7$  kcal mol<sup>-1</sup> in: Reiner, J.; Watts, R.; Klein, M. *Chem. Phys.* **1982**, *64*, 95.
- (30) Feyereisen, M. W.; Feller, D.; Dixon, D. A. *J. Phys. Chem.* **1996**, *100*, 2993.
- (31) DeMore, W. B.; Sander, S. P.; Golden, D. M.; Hampson, R. F.; Kurylo, M. J.; Howard, C. J.; Ravishankara, A. R.; Kolb, C. E.; Molina, M. J. *Chemical Kinetics and Photochemical Data for Use in Stratospheric Modeling*; JPL Publication 94-26, NASA, 1994.
- (32) Shepson, P. B. Private communication.
- (33) Nelander, B. *J. Phys. Chem. A* **1997**, *101*, 9092.